



Universiteit
Leiden
The Netherlands

Nanofluidic tools for bioanalysis : the large advantages of the nano-scale

Janssen, K.G.H.

Citation

Janssen, K. G. H. (2013, December 19). *Nanofluidic tools for bioanalysis : the large advantages of the nano-scale*. Retrieved from <https://hdl.handle.net/1887/22946>

Version: Corrected Publisher's Version

License: [Licence agreement concerning inclusion of doctoral thesis in the Institutional Repository of the University of Leiden](#)

Downloaded from: <https://hdl.handle.net/1887/22946>

Note: To cite this publication please use the final published version (if applicable).

Cover Page



Universiteit Leiden



The handle <http://hdl.handle.net/1887/22946> holds various files of this Leiden University dissertation

Author: Janssen, Kjeld G.H.

Title: Nanofluidic tools for bioanalysis : the large advantages of the nanoscale

Issue Date: 2013-12-19

Single-Electrolyte Isotachophoresis Using a Nanochannel-Induced Depletion Zone^a

4.1 Abstract

Isotachophoretic separations are triggered at the border of a nanochannel-induced ion-depleted zone. This depletion zone acts as a terminating electrolyte and is created by concentration polarization over the nanochannel. We show both continuous and discrete sample injections as well as separation of up to four analytes. Continuous injection of a spacer compound was used for selective analyte elution. Zones were kept focused for over one hour, while shifting less than 700 μm . Moreover, zones could be deliberately positioned in the separation channel and focusing strength could be precisely tuned employing a three-point voltage actuation scheme. This makes depletion zone isotachophoresis (dzITP) a fully controllable single-electrolyte focusing and separation technique. For on-chip electrokinetic methods, dzITP sets a new standard in terms of versatility and operational simplicity.

^aPublished as: Jos Quist[†], Kjeld G. H. Janssen[†], Paul Vulto, Thomas Hankemeier and Heiko J. van der Linden, *Analytical Chemistry*, **83**, 7910-7915 (2011)

[†] Equally contributing authors.

4.2 Introduction

Isotachopheresis (ITP) is a powerful electrokinetic technique for the concentration, separation, purification and quantification of ionic analytes, especially when downscaled to microfluidic devices^{33,131}. In 1998, Walker et al. were among the first to demonstrate on-chip ITP using Raman spectroscopy to detect herbicides⁶¹. Kanianski et al. coupled ITP to capillary electrophoresis (CE) on a chip and showed isotachopherograms of up to 14 analytes¹³². Several reports describe over 10,000-fold concentration^{133–135}. Jung et al. even reported millionfold sample stacking using transient ITP⁵⁷. Miniaturized ITP is applicable to a broad range of samples, including toxins from tap water⁵⁹, explosive residues¹³⁶, proteins¹³⁷, DNA from PCR samples^{138,139}, nucleic acids from whole blood¹⁴⁰ and small RNA molecules from cell lysate¹⁴¹. Hybridization of RNA's with molecular beacons by ITP¹⁴² was applied to bacterial rRNA's from urine¹⁴³, demonstrating the potential of on-chip ITP for biochemical assays. A major recent achievement was the integration of an ITP chip and laser-induced-fluorescence (LIF) detection into a single handheld device¹⁴⁴. Nevertheless, ITP has still to come to its full potential, as until now it has not been widely used for bioanalytical applications^{145–147}. A major limitation is that ITP requires a sample to be injected between a leading electrolyte and a terminating electrolyte. Compared to e.g. capillary electrophoresis (CE), which uses a single electrolyte only, handling and method development is not straightforward. Another limitation of conventional ITP is that analyte zone positions are difficult to control. This is due to the different conductivities of the ITP zones, resulting in continuous changes of electric field distributions during electromigration. Several stationary ITP strategies have been developed to alleviate this limitation. One such strategy employs a hydrodynamic counterflow, but this has the disadvantage of dispersion due to a parabolic flow profile¹⁴⁸. A more elegant strategy is balancing the electrophoretic motion of the ITP zones by an opposite electro-osmotic flow (EOF)^{149–152}. However, with this method it is still complicated to change analyte zone positions in a controlled manner without changing pH or electrolyte concentrations.

In this paper we overcome the mentioned limitations by a radically different approach which combines the strengths of on-chip ITP with the merits of nanofluidic concentration devices^{65,153}. These devices, which have been extensively reviewed by Kim et al.⁶⁸, are in fact miniaturized variants of electrocapture devices. Electrocapture is a powerful method which utilizes capillaries with perm-selective membrane junctions for trapping and selective release of ionic compounds^{154,155}. In nanofluidic concentration devices, at least two parallel microchannels are connected by a nanochannel, over which an electric field is applied (Figure 4.1a). Asymmetric distribution of anions and cations^{107,156} makes the nanochannel perm-selective, leading to concentration polarization^{49,50,157}. This causes the formation of a depletion zone in the anodic microchannel. A tangential EOF through this microchannel transports analytes towards the border of the depletion zone, where they are trapped (Figure 4.1b). Various groups

have investigated devices based on similar principles^{51,158–163}, showing that this has become a very active research field within a short time. Potential applications include immunoassays^{164–167}, enzyme assays^{167–169}, massive parallelization^{170,171} and desalination¹⁷². Here we employ a depletion zone to induce isotachopheretic separations. To our knowledge, this is the first time such separations are demonstrated in nanofluidic concentration devices. Depletion zone isotachopheresis (dzITP), as we coin this novel approach, is performed with a single electrolyte only. A three-point voltage actuation scheme gives complete control over the position of the zones and the sharpness of their borders, utilizing the fact that the method is quasi-static. The simplicity and versatility of our method makes it a powerful new tool in the electrokinetic focusing and separation toolkit.

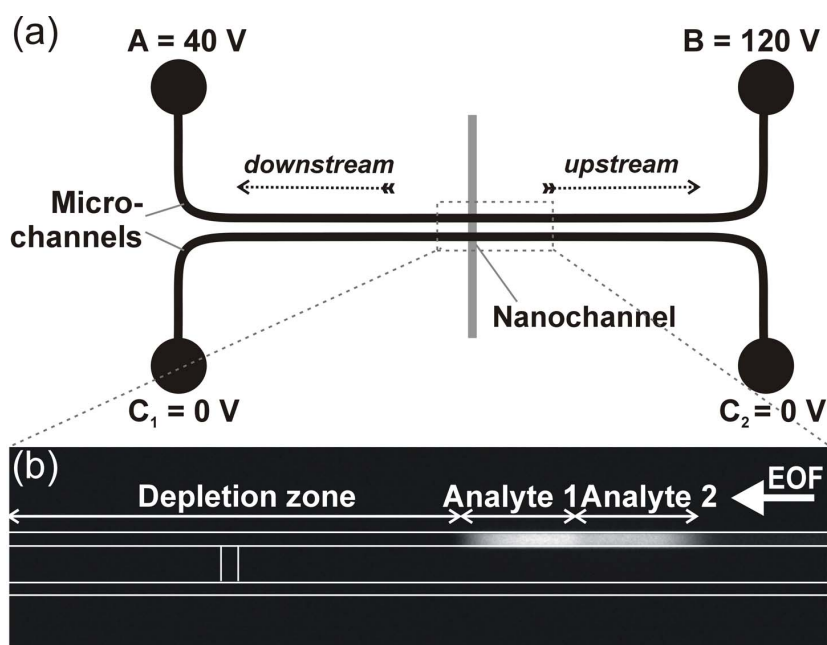


Figure 4.1 a) Chip layout consisting of two microchannels and one nanochannel. An example of three-point voltage actuation is provided: A is the downstream voltage, B the upstream voltage, while the lower channel is connected to ground, as represented by voltages $C_{1,2} = 0 \text{ V}$. Downstream and upstream directions are indicated by dashed arrows. b) Example of dzITP separated zones. The channel contains a depletion zone that extends mostly in the downstream channel. Analytes focus at the border of the depletion zone and order themselves in clearly distinguishable zones. Lines that indicate micro- and nanochannels were drawn onto the CCD image.

4.3 Experimental

4.3.1 Chemicals

Lithium carbonate was obtained from Acros Organics (Geel, Belgium); disodium fluorescein was obtained from Riedel-de Haën (Seelze, Germany); 6-carboxy-fluorescein was obtained from Sigma-Aldrich (Steinheim, Germany); and sodium acetate was obtained from Merck (Darmstadt, Germany). FITC-labeled amino acids were synthesized as described in Section 3.7.1. In all experiments, 2.0 mmol/L lithium carbonate, pH 10.6 was used as the background electrolyte. Solutions were prepared fresh before experiments.

4.3.2 Chip preparation

Chips were fabricated in Pyrex® wafers using standard lithography techniques and deep reactive ion etching (DRIE). The chip fabrication procedure is described in detail in the appendix Section 4.7.2. The microchannels had 1.7 μm depth and 20 μm width. Microchannel lengths between fluid reservoirs and the nanochannel were 0.91 cm. The nanochannel that connected the two microchannels was 60 nm deep, 25 μm wide and 50 μm long. The chip was prefilled with ethanol to eliminate air trapping, after which the chip was flushed at least 15 minutes with 100 mmol/L NaOH, 15 minutes with demineralized water and 15 minutes with background electrolyte (2.0 mmol/L lithium carbonate). Fluid replacement and flushing was accomplished by leaving the fluid reservoir at one end of a microchannel empty. A combination of capillary action and evaporation of fluid generated a flow which was sufficient to replace all fluid in a microchannel in approximately 3 minutes. Reservoirs were washed 3 times after fluid replacement. After flushing, all channels and reservoirs were filled with the background electrolyte (2.0 mmol/L lithium carbonate).

4.3.3 Setup and microscopy

Access holes were extended with fluidic reservoirs (volume 100 μL) using a custom-build interface that was attached to the chip surface using a vacuum. The fluidic reservoirs were electrically connected using gold electrodes. Two power supplies (ES 0300 045, Delta Elektronika BV, Zierikzee, The Netherlands) were controlled via the analog outputs of an NI USB 6221 data acquisition system using LabVIEW 8.2 software (National Instruments, Austin, TX). For fluorescence microscopy, an Olympus IX71 microscope (Olympus, Zoeterwoude, The Netherlands) was used in combination with an Hamamatsu Orca-ER digital camera and Hokawo version 2.1 imaging software (Hamamatsu Photonics, Nuremberg, Germany). The magnification was 40x. To minimize photobleaching, low lamp intensities were combined with 1.0 second integration times.

4.3.4 Data processing

Spatiotemporal plots (Figure 4.2) were composed using MATLAB®, by adjoining fluorescence profiles obtained from image sequences that were recorded during the experiments. Fluorescence profiles were obtained by averaging 50 image lines and correcting them for background signal. False colors were assigned to represent fluorescence intensity. Raw CCD images were used in Figure 4.3. Fluorescence profiles were obtained from the CCD images and were smoothed by averaging over 5 pixels. Slope values were determined at the inflection points of the smoothed profiles and normalized with respect to the maximum intensity value of the corresponding analyte zone. Locations of the edges of the zones were obtained by determining the position of the inflection point relative to the upstream edge of the nanochannel.

4.4 Results and Discussion

4.4.1 Device operation

4.1a and b show the general device operation for dzITP. The upper channel in Figure 1a, b is the separation channel, this is the channel where isotachophoretic zones are formed during the experiment. Three-point voltage actuation is utilized: to each of the access holes of the separation channel a voltage source is connected, while the other channel is connected to ground. Upon voltage application, concentration polarization takes place: an ion depletion zone forms in the separation channel, while in the other channel an ion enrichment zone forms (not shown here, see ref. 29). Asymmetric voltage application over the separation channel yields an EOF through this channel. The channel arm between the higher voltage and the nanochannel is referred to as the "upstream channel", while the arm between the lower voltage and the nanochannel is referred to as the "downstream channel" (see Figure 1a). Downstream, the depletion zone continues to grow until the fluid reservoir is reached. This process sometimes appears to lead to fluctuations during the first 30-60 seconds of an experiment. In the upstream direction, depletion zone growth becomes balanced by the opposing EOF. When the downstream depletion zone reaches the outlet, the electrical resistance in this channel reaches a more stable value, resulting in a near-stable position for the upstream depletion zone border. At this border, analytes are focused based on a difference in ion density (for detailed theory see Zangle et al.⁵⁰). Meanwhile, analyte concentration and separation into adjacent zones is achieved according to isotachophoretic principles (see Figure 4.1b). The depletion zone serves here as a terminating electrolyte, the background electrolyte takes the function of the leading electrolyte. They define the ionic mobility window of analytes that can be focused. The upper boundary of this mobility window is defined by the mobility of the leading ion in the background electrolyte: analytes with higher mobilities will

be transported towards the reservoir. The lower boundary depends on the electric field in the depletion zone, which is very high. For example, Kim et al measured a 30-fold amplified electric field in the depletion zone¹⁷³. Only analytes with very low mobilities are transported through this barrier by EOF transport.

As the current setup is based on a glass chip, the channels have a negative surface charge. Consequently, only anions are focused and separated at the depletion zone border. In order to enable focusing and separation of cations, the surface charge of the device should be reversed by applying a surface coating or by choosing a different substrate.

4.4.2 Discrete and continuous injections

dzITP is demonstrated for both discrete and continuous injections (see Figure 4.2a, b). Fluorescein, 50 $\mu\text{mol/L}$ and 6-carboxyfluorescein, 50 $\mu\text{mol/L}$ were used as analytes; applied voltages were 120 V (upstream) and 40 V (downstream). For discrete injections, only the separation channel was filled with sample, while remaining channels and fluid reservoirs contained background electrolyte only. This resulted in a 309 pL injection volume, as calculated from the microchannel dimensions. Figure 4.2a shows that isotachopheretic separation continues until all analytes from the discrete sample are focused, after which the zone widths become constant. Over time, bending points can be observed in the growth rate of the analyte zones, as indicated by the arrows in Figure 4.2a. These bending points correspond to the exhaustion of fluorescein (arrow I) and 6-carboxyfluorescein (arrow II). Lower mobility compounds are exhausted at an earlier stage than compounds of higher mobility, the reason being that lower mobility compounds have a lower electrophoretic drift to counter the EOF, resulting in a higher net velocity. In continuous injections, the analytes were also placed in the upstream fluid reservoir, providing a practically inexhaustible supply of analytes. Therefore zone broadening was continuous (see Figure 4.2b). Clearly, no bends due to analyte exhaustion were present. Zone broadening speed of the lower mobility compound (fluorescein) is higher than for the higher mobility compound (6-carboxyfluorescein), again due to a higher net velocity. Continuous injections are therefore most advantageous for the extraction and focusing of low-concentration, low-mobility analytes, while discrete injections are useful in the quantitative analysis of multiple analytes.

4.4.3 Four-compound separation

4.2c shows concentration and separation of four compounds. A discrete sample containing fluorescein, 6-carboxyfluorescein, FITC-leucine and FITC-glutamate, 40 $\mu\text{mol/L}$ each, was injected. External voltages were 120 V (upstream) and 40 V (downstream). Within 100 seconds, four zones of clearly distinguishable fluorescence intensity were formed. Standard addition was used to assign the

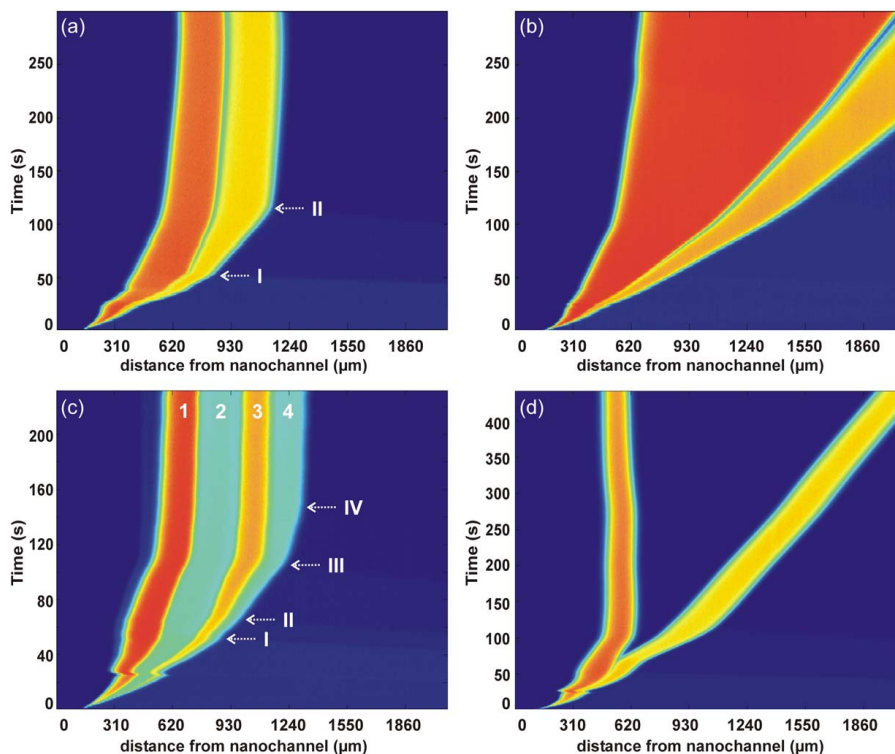


Figure 4.2 Spatiotemporal plots of dzITP separations. a) Discrete injection of fluorescein and 6-carboxyfluorescein. Arrows I and II indicate exhaustion of fluorescein and 6-carboxyfluorescein respectively. b) Continuous injection of fluorescein and 6-carboxyfluorescein. c) Discrete injection and separation of four compounds: fluorescein (1), FITC-leucine (2), 6-carboxyfluorescein (3) and FITC-glutamate (4). Arrows I-IV indicate exhaustion of these respective analytes. d) Discrete injection of fluorescein and 6-carboxyfluorescein combined with a continuous injection of acetate.

four zones to each of the four analytes: a doubled concentration of the respective analyte led approximately to a doubling of the width of the corresponding zone (see appendix 4.7.3). Here, too, bends in the profile coincide with the exhaustion of each of the respective analytes.

4.4.4 Spacer compounds

A combination of a continuous and a discrete injection is shown in Figure 4.2d. The upstream fluid reservoir was filled with electrolyte containing 100 μmol/L sodium acetate as a spacer compound, but no analytes. The separation channel was filled with electrolyte containing 30 μmol/L of both fluorescein and 6-carboxyfluorescein as analytes, but no spacer compound. External voltages were 120 V (upstream) and 40 V (downstream). Initially, fluorescein and 6-carboxyfluorescein

are focused in adjacent zones. After 70 seconds, acetate, which has an ionic mobility in between that of fluorescein and 6-carboxyfluorescein, arrives and spaces the two compounds. The fluorescein zone remains focused at the depletion zone border, while the 6-carboxyfluorescein zone is pushed away in upstream direction by the continuously broadening acetate zone. Spacer addition enables baseline separation of fluorescent compounds enabling more precise identification and quantification. Furthermore, a single compound or a specific group of compounds can be selectively transported away from the depletion zone and can eventually be eluted from the system, while other compounds remain at their near-stationary position at the border of the depletion zone. Advantageously, all compounds remain focused during this process. Thus, spacer addition is a powerful method for purification and transport.

4.4.5 Positional stability

A crucial feature of dzITP is the positional stability of the depletion zone border. A near-stationary condition is reached after a rather short period, typically in the order of 100 seconds (see Figure 4.2), in which depletion rate and EOF velocity reach a balance. A discrete injection experiment was performed with 50 $\mu\text{mol/L}$ of both fluorescein and 6-carboxyfluorescein; external voltages were 120 V (upstream) and 40 V (downstream). In this experiment, the depletion zone border shifted less than 700 μm in 1 hour. A previous report on nanofluidic concentration devices indicated a near-zero shift after 3 hours of actuation⁶⁵, although under different experimental conditions, indicating that the result reported here could be further optimized. However, the near-stability of the isotachopheretic separations demonstrated here greatly enhances monitoring of focusing and separation processes by microscopy without x/y control of the microscope stage. Additionally, the experimental time range is much larger than for non-stationary ITP methods, allowing higher concentration factors to be achieved.

4.4.6 Three-point voltage actuation

In 4.3 we demonstrate the versatility that is provided by a three-point voltage actuation approach. In Figure 4.3a and b the magnitude of the upstream and downstream voltages was varied, while maintaining the ratio between them. This enables tuning of the extent to which analytes are focused. For low voltages the two zones are barely distinguishable, while for high voltages sharp edges of the zones can be observed. Figure 4.3b shows normalized slope values in fluorescence intensity per μm . The results suggest a linear trend between voltage magnitude and zone sharpness. Analyte zone positions are not greatly influenced by a change of the voltage magnitude as long as the ratio between upstream and downstream voltages is kept constant. In principle this enables a free choice of the maximum field strength and resulting focusing strength. However, small shifts

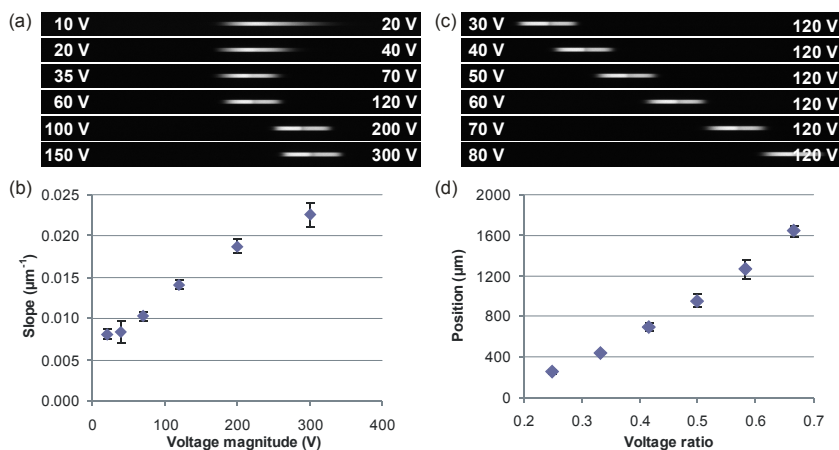


Figure 4.3 Three-point voltage actuation. a) Focusing and separation of fluorescein and 6-carboxyfluorescein at several voltage magnitudes. b) Dependence of focusing strength on the voltage magnitude. Focusing strengths are represented by the steepness of the slopes between the fluorescein plateau and the depletion zone; voltage magnitudes are represented by the upstream voltage. c) Fluorescein and 6-carboxyfluorescein zones at different ratio's between upstream and downstream voltages. d) Distances of the edge between the depletion zone and the fluorescein zone from the nanochannel. Measurements were triplicated and randomized.

in analyte zone positions are observed at higher voltage magnitudes. We measured maximum shifts of $364 \pm 21 \mu\text{m}$. In Figure 4.3c and d the voltage ratio is varied by means of the downstream voltage. The zones can be shifted over a range of 1.4 mm by varying the voltage ratio between 0.25 and 0.67 (downstream voltage : upstream voltage). Zone positions appear to relate rather linear to the voltage ratio. Separations are maintained, although at increasing ratios defocusing occurs. The 1.4 mm zone shift is accompanied by a decrease of slope values in the order of $0.006 \mu\text{m}^{-1}$.

Complete control over analyte zone position and sharpness is a crucial and unique advantage of dzITP over conventional ITP methods. In conventional methods, a single stable position can be obtained by EOF balancing, but during the experiment this position can not be easily changed without changing parameters like pH or electrolyte concentrations. Contrarily, in dzITP this is easily done by tuning the upstream and downstream voltage magnitudes. Real-time image analysis of fluorescent markers can be used as feedback input for three-point voltage actuation, enabling automated zone positioning control. Moreover, great benefit is offered to experimental readout, as analyte zones can be scanned in a precisely controllable manner by steering them along a sensor.

Table 4.1 Comparison of dzITP with conventional ITP methods and nanofluidic concentration devices (NCD). ✓ = intrinsic or standard possibility; - = not possible or not demonstrated in literature; m = possible with modification.

Property	ITP	NCD	dzITP
analyte focusing	✓	✓	✓
separation of ions	✓	-	✓
spacer insertion	✓	-	✓
single electrolyte	-	✓	✓
near-stationary	m	✓	✓
voltage controlled zone positioning	-	-	✓

4.4.7 Synergy of dzITP

Table 1 summarizes the synergy that emerges from the combination of ITP and nanofluidic concentration devices, as provided by dzITP. Except for the requirement of multiple electrolytes, dzITP has all key characteristics of ITP: focusing towards plateau concentrations and separation into adjacent zones that are ordered according to ionic mobility. Spacer compounds can be used to segregate adjacent zones. From nanofluidic concentration devices, dzITP takes the single-electrolyte advantage, as well as positional stability. Three-point voltage actuation adds to this synergy the possibility of precise control of focusing strength and zone positioning.

4.5 Conclusion and Outlook

In this paper we have demonstrated isotachophoretic separations employing a nanochannel-induced depletion zone as a trailing electrolyte. dzITP requires only a single background electrolyte to be injected and can be performed easily with both discrete and continuous injections. We demonstrated separations of up to four compounds in clearly distinguishable zones within 100 seconds. A spacer was inserted to improve baseline separation of fluorescent compounds, and to induce selective transport of analytes while maintaining sharply focused zones. Moreover, full control over analyte position and zone sharpness was demonstrated using the unique three-point voltage control of dzITP. Scanning of analyte zones using three-point voltage actuation will enable simple integration of sensors such as surface-enhanced Raman spectroscopy (SERS), surface plasmon resonance (SPR), and conductimetry or electrochemical detection. As dzITP is much easier to use than conventional ITP, integration into a microfluidic platform for everyday laboratory use will be very attractive, as exemplified by the Agilent 2100 Bioanalyzer for on-chip capillary electrophoresis. Integration in hand-held anal-

ysis devices, as has been recently done for conventional ITP¹⁴⁴, may find interesting applications in water quality monitoring, explosive detection, point-of-care screening, etc. Future research focuses on coupling of the technique to sampling and detection modules. We see great potential for dzITP in our metabolomics research, particularly for the extraction, preconcentration and quantification of low-abundant metabolites from small complex biological samples. Thanks to its unique combination of voltage-controlled versatility and single-electrolyte simplicity, dzITP holds the promise to become a core component in the electrokinetic chip-based platforms of the future.

4.6 Acknowledgements

We thank Marcel Hesselberth, Daan Boltjes (Leiden Institute of Physics, Leiden University), Jiajie Li (LACDR, Leiden University) and Stefan Schlautmann (MESA+, Twente University) for helpful discussions and support with device fabrication. We thank Richard van den Berg (Leiden Institute of Chemistry, Leiden University) for assistance on the synthesis of FITC-labeled amino acids and Raphaël Zwier (Fine-Mechanical Department, Leiden University) for constructing the chip interface. This project was financed by the Netherlands Metabolomics Centre, the Netherlands Genomics Initiative and the Netherlands Organization for Scientific Research (NWO).

4.7 Appendix

4.7.1 Additional movies

Several movies are available in the electronic supporting information online with the publication belonging to this chapter¹⁷⁴: Movie 1: dzITP-separation after a discrete injection of four compounds: fluorescein, FITC-leucine, 6-carboxyfluorescein and FITC-glutamate. Movie 2: Discrete injection of fluorescein and 6-carboxyfluorescein combined with a continuous injection of acetate as a spacer. Movie 3: Fluorescein and 6-carboxyfluorescein zones are positioned by using different ratios between upstream and downstream voltages.

4.7.2 Chip fabrication

Photoresists (SU 8-10 and ma-P 1275) and developers (mr-Dev 600 and ma-D 331) were obtained from Microresist Technologies (Berlin, Germany). N-methylpyrrolidone (NMP) was obtained from Rathburn Chemicals (Walkerburn, Scotland). AbsorbMaxTM film, fuming nitric acid (100%) and hexamethyldisilazane (HMDS) were obtained from Sigma-Aldrich (Steinheim, Germany). Chips containing micro- and nanochannels were fabricated in 4" Pyrex® wafers (Si-Mat,

Kaufering, Germany). The wafers were spin coated with SU 8-10; the wafer was first accelerated to 500 rpm in 5 seconds to allow resist spreading, directly followed by an acceleration to 2000 rpm in 5 seconds, which was maintained for 30 seconds. After spin coating, the resist was allowed to settle for 8 hours at room temperature, after which the resist was prebaked using a hotplate by controlled heating to 95 °C in 8 minutes, followed by ambient cool down. The resist was exposed at 6 mW/cm² for 25 seconds in a Suss MA 45 mask aligner (Karl Suss KG, München-Garching, Germany) in which a Hoya UV34 filter (LG optical, Churchfield, UK) was installed to prevent SU 8 T-topping. During exposure AbsorbMax film was attached to the back side of the wafer, to prevent undesired reflections. The microchannel pattern was transferred using a 5" chromium mask (Delta Mask, Enschede, The Netherlands). A post-exposure bake was done by controlled heating to 95 °C in 8 minutes, followed by ambient cool down. Development was done for 3 minutes in mr-Dev 600 developer followed by washing in isopropanol and demineralized water. Using the developed SU 8 resist as a mask, microchannels were etched into the glass wafers by a 1 hour deep reactive ion etching (DRIE) step. DRIE was performed in an Oxford Plasmalab 90+ parallel plate reactor (Oxford Instruments, Abingdon, United Kingdom) using an argon/SF₆ plasma. Gas flows were 20 sccm for argon and 25 sccm for SF₆. After establishing a stable plasma at 10 mTorr, pressure was set at 2 mTorr. Forward power was 200 W. After etching, the SU 8 resist was stripped by placing the wafers in NMP for several hours at 70 °C, followed by removal of remaining particles in a fuming nitric acid bath. The wafers were rinsed in water, spin-dried, and baked for 5 minutes at 110 °C for dehydration. The wafers were spin coated with HMDS followed by a curing bake at 150 °C for 5 minutes. Next, ma-P resist was spin coated at 1000 rpm for 30 seconds preceded by 10 seconds of acceleration. The resist was prebaked for 5 minutes at 95 °C. Transfer of the nanochannel pattern was performed by an exposure step as performed as described above. Development was done with ma-D 331 developer for 5 minutes. To etch the nanochannels, DRIE was performed with same parameters as described above, except for the etch time, which was 100 seconds. The ma-P resist was stripped with acetone. Resulting micro- and nanochannel depths were 1.7 μm and 60 nm respectively, as measured with a Dektak 150 profilometer (Veeco, Tucson, AZ) and by scanning electron microscopy using a FEI NovaTM NanoSEM apparatus (FEI, Hillsboro, OR). Each etched wafer was bonded with a second pyrex® wafer. In these wafers, fluidic access holes were ultrasonically drilled using a diamond bit. Both wafers were subsequently cleaned in acetone, piranha acid and nitric acid, followed by a 1 minute dip in KOH. A pre-bond was realized upon application of manual pressure, after which direct bonding was performed in an oven (Model P320, Nabertherm GmbH, Lilienthal, Germany). The temperature was ramped to 600 °C in 3 h, which temperature was maintained for 4 h, followed by cooling to room temperature with a rate of 50 °C/h. After bonding, wafers were not diced, a whole wafer was used from which a single chip was selected.

4.7.3 Analyte zone identification by standard addition

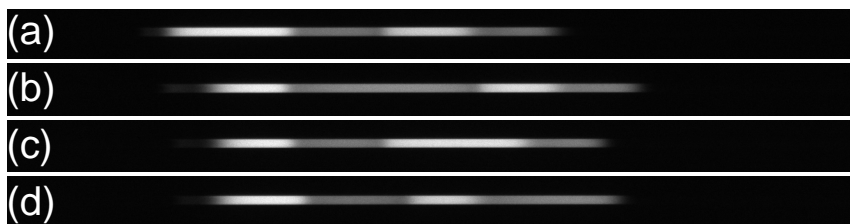


Figure 4.4 Analyte zone identification by standard addition. In each experiment, the four analytes (fluorescein, FITC-leucine, 6-carboxyfluorescein and FITC-glutamate) were present in concentrations of 30 $\mu\text{mol/L}$, except for the analyte to be identified, which had a concentration of 60 $\mu\text{mol/L}$. Discrete injections were performed. From left to right, the four zones were identified as follows: a) first zone: fluorescein; b) second zone: FITC-leucine; c) third zone: 6-carboxyfluorescein; d) fourth zone: FITC-glutamate.

